Accepted Manuscript

Localized magnetic state in the Rashba model

H.O. Frota, M.S. Gusmão, Angsula Ghosh

Please cite this article as: H.O. Frota, M.S. Gusmão, A. Ghosh, Localized magnetic state in the Rashba model, *Physica B: Physics of Condensed Matter* (2018), doi: https://doi.org/10.1016/j.physb.2018.11.002.
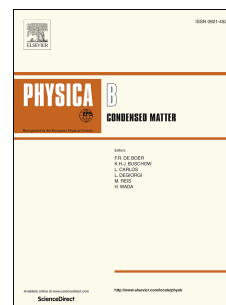
Localized Magnetic State in the Rashba Model

H. O. Frota, M. S. Gusmão, Angsula Ghosh*

Department of Physics, Federal University of Amazonas, 69077-000 Manaus, AM, Brazil

Abstract

We study the formation of local moments in a metallic host due to a localized spin-orbit (Rashba) interaction. Using the Anderson model we describe the occurrence of magnetic moments through calculation of the magnetic-non-magnetic phase transition within the mean-field scenario. We compare our results with those in the absence of the Rashba interaction. The symmetry and regime of the magnetic phase demonstrates a dependence on the above interaction. The conductance values through the impurities are also exhibited for the above phases.

Keywords: Magnetic impurity, spin-orbit, Rashba interaction

1. Introduction

Spintronics that involves manipulation of spin degrees of freedom plays a determining role in solid state devices. Spin logics not only helps in power saving but are also highly useful due to its portability and non-volatility [1]. Both metal spintronics and semiconductor spintronics have fascinated the scientific community for years. Materials that demonstrate magnetism and high spin–orbit interaction are promising candidates for spintronic devices. The phenomenon finds it use in various technological applications. It has made possible the huge increase in the storage capacity and helped create the information-based world of today [2]. Spin degrees of freedom are also deployed to convert heat to energy through spin-Seebeck effect thereby leading to a new area of research called spin-caloritronics [4, 5] important in information processing, communications and biologically inspired computing. Various application of spintronics have also been predicted in magnonics [6], microwave detectors [7] and magnetic field sensing [8]. Spintronic sensors are highly advantageous due to the reduced cost, small dimensions and high magnetic-field sensitivity and are utilized in various industrial applications like magnetic compass [9], current sensors [10], DNA and protein biochips[11], neuronal magnetic field probing [12] etc.

---

*Corresponding author

Email address: angsula@ufam.edu.br (Angsula Ghosh)

Metal spintronics has already proved to be essential in the computer industry [3]. Spintronics in ferromagnetic metals [13, 14], anti-ferromagnetic metals [15–19] have been widely studied. Recently spintronics devices made of low-cost metals and silicon [20] originating from Rashba spin-orbit coupling due to structure inversion asymmetry at the interface could motivate the awakening of silicon spintronics devices.

Semiconductor spintronics has been fascinating and fundamental to investigate the transport. However, we are far away in understanding this phenomenon to its full potential. The recent studies on spin Hall effects, both extrinsic [21, 22] and intrinsic [23], have paved the ways to extensive studies on the subject [24]. The spin-orbit coupling, most fundamental spin-dependent interaction, induced by the presence of impurities or by the intrinsic lattice itself gives rise to the spin currents suitable for spintronics devices.

The effect of the the spin-orbit coupling in heterostructures of different multifunctional materials have paved its way to a new field denominated as "spin orbitronics" [25, 26]. A spin-polarized field effect transistor based on the Rashba interaction has motivated various works in narrow gap semiconductors where the gate voltage of the device could be used to modulate the above interaction [27]. The Rashba spin-orbit interaction has been predominantly fundamental in spintronics as can be seen in inverted heterostructures [28], four probe (beam-splitter) geometry [29] as well as In As based heterostructures [30–33]. The experimental data [34] on few-electron quantum dots have been considered in terms of Rashba spin-orbit coupling and exchange interaction [35]. The correlation effects in few-electron lateral quantum dot in a fully interacting Hamiltonian of electrons confined in a quantum dot [36, 37] have attracted a lot of attention. Rashba dots in a metallic host in the presence of Coulomb interaction was considered to investigate the transport properties [38, 39] using the Anderson Hamiltonian.

In this work we consider the magnetic-non-magnetic phase transition of the impurity in a metallic host with the Rashba interaction. The Anderson model for magnetic impurities in a metallic host has been studied to investigate the formation of the local moment in the presence of the Rashba interaction. An onsite Coulomb interaction has been responsible for the magnetic ordering. Parameters of the Rashba interaction modifies the phase diagram of the impurity and the regions favorable for the presence of the spin filter properties. The paper is organized is as follows. In section II, the Anderson impurity model [40] has been discussed whereas the Green's function technique within the mean field scenario utilized for our work is detailed in section III. In section IV the phase space along with the occupation numbers and the conductance values are discussed. Finally a short summary on our results is depicted in section V.

2. Model

The model Hamiltonian is given by

$$H = H_R + H_f + H_V \tag{1}$$

2

where

$$H_R = \sum_{\vec{k}} \varepsilon_{\vec{k}} c^{\dagger}_{\vec{k}\nu} c_{\vec{k}\nu} - \alpha_R \sum_{\vec{k}} |\vec{k}| \left(e^{i\theta} c^{\dagger}_{\vec{k}\uparrow} c_{\vec{k}\downarrow} + e^{-i\theta} c^{\dagger}_{\vec{k}\downarrow} c_{\vec{k}\uparrow} \right) \qquad (2)$$

$$H_V = V \sum_{\vec{k}} \left(c^{\dagger}_{\vec{k}\nu} c_{f\nu} + c^{\dagger}_{f\nu} c_{\vec{k}\nu} \right) \qquad (3)$$

$$H_f = \varepsilon_f c^{\dagger}_{f\nu} c_{f\nu} + U c^{\dagger}_{f\uparrow} c_{f\uparrow} c^{\dagger}_{f\downarrow} c_{f\downarrow}, \qquad (4)$$

repeated index (ν) means summation over that index, $c^{\dagger}_{\vec{k}\nu} (c_{\vec{k}\nu})$ creates (annihilates) an electron in the conduction band with momentum $\vec{k}$ in the xy plane, spin ν and energy $\varepsilon_{\vec{k}}$, α_R is the Rashba constant, θ is the angle between $\vec{k}$ and the y-axis, $c^{\dagger}_{f\nu}(c_{f\nu})$ creates (annihilates) an electron with spin ν and energy ε_f in the impurity orbital, inside which two electrons interact each other with the Coulomb energy U, and V is the hybridization energy between the conduction band and the impurity orbital. Eq. (2) can be written in terms of the operators

$$a_{\vec{k}\pm} = \frac{1}{\sqrt{2}} \left(c_{\vec{k}\uparrow} \pm i e^{i\theta} c_{\vec{k}\downarrow} \right), \qquad (5)$$

which obeys the fermion anticommutation relations $\{a_{\vec{k}\gamma}, a^{\dagger}_{\vec{k}'\gamma'}\} = \delta_{\vec{k}\vec{k}'} \delta_{\vec{k}'\gamma'}$ ($\gamma = \pm$), and diagonalizes H_R, whose eigenvalues are given by

$$\xi_{\vec{k}\pm} = \frac{\hbar^2}{2m} (k + \gamma k_R)^2 - \xi_R, \qquad (6)$$

with $k = |\vec{k}|$, $\xi_R = (\hbar^2/2m) k_R^2$ and $k_R = m\alpha_R/\hbar^2$. Analogous to Eq. (5), the fermionic $f_{\pm}$ operators are introduced,

$$f_{\pm} = \frac{1}{\sqrt{2}} \left(c_{f\uparrow} \pm i e^{i\theta} c_{f\downarrow} \right). \qquad (7)$$

In the mean field approach the Hamiltonian H_f is written as $H_f = \varepsilon_{f\nu} c^{\dagger}_{f\nu} c_{f\nu}$, where $\varepsilon_{f\nu} = \varepsilon_f + U \left\langle c^{\dagger}_{f-\nu} c_{f-\nu} \right\rangle$. In terms of the operators $a_{\vec{k}\gamma}$ and f_{γ}, the total Hamiltonian H, given by Eq. (1), acquires the form

$$H = \sum_{\vec{k}} \xi_{\vec{k}\gamma} a^{\dagger}_{\vec{k}\gamma} a_{\vec{k}\gamma} + V \sum_{\vec{k}} \left(a^{\dagger}_{\vec{k}\gamma} f_{\gamma} + f^{\dagger}_{\gamma} a_{\vec{k}\gamma} \right) + \Delta_+ f^{\dagger}_{\gamma} f_{\gamma} + \Delta_- (f^{\dagger}_+ f_- + f^{\dagger}_- f_+), \quad (8)$$

where $\Delta_{\pm} = (\varepsilon_{f\uparrow} \pm \varepsilon_{f\downarrow})/2$, representing a two channel system which communicates with each other via Δ_-.

3. The Formalism

In this section the Green function formalism used in the work is presented. The retarded Green function is given by $G^R(c_{f\nu}; t - t')$,

3

$$G^R(c_{f\nu}; t - t') = -i\theta(t - t')\left\langle\{c_{f\nu}(t), c_{f\nu}^\dagger(t')\}\right\rangle, \qquad (9)$$

which rewritten in terms of the operator f_γ, as in Eq. (7), assumes the form

$$G^R(c_{f\uparrow}; t - t') = \frac{1}{2}\sum_{\gamma\gamma'}G^R(f_\gamma f_{\gamma'}; t - t') \qquad (10)$$

$$G^R(c_{f\downarrow}; t - t') = \frac{1}{2}\sum_{\gamma\gamma'}\epsilon_\gamma\epsilon_{\gamma'}G^R(f_\gamma f_{\gamma'}; t - t'), \qquad (11)$$

with

$$G^R(f_\gamma f_{\gamma'}; t - t') = -i\theta(t - t')\left\langle\{f_\gamma(t), f_{\gamma'}^\dagger(t')\}\right\rangle \qquad (12)$$

and $\epsilon_\pm = \pm 1$.

The Green functions given by Eq. (12) is obtained using the equation of motion method. Hence,

$$G^R(f_\gamma f_\gamma, \omega) = \left[\omega - \Delta_+ - \Sigma^\gamma(\omega) - \frac{\Delta_-^2}{\omega - \Delta_+ - \Sigma^{-\gamma}(\omega)}\right]^{-1} \qquad (13)$$

$$G^R(f_\gamma f_{-\gamma}, \omega) = \frac{\Delta_-}{\omega - \Delta_+ - \Sigma^\gamma(\omega)}\left[\omega - \Delta_+ - \Sigma^{-\gamma}(\omega) - \frac{\Delta_-^2}{\omega - \Delta_+ - \Sigma^\gamma(\omega)}\right]^{-1}, \qquad (14)$$

where $\Sigma^\gamma(\omega)$ represents the self energy given by

$$\Sigma^\gamma(\omega) = \sum_{\vec{k}}\frac{V^2}{\omega + i\eta - \xi_{\vec{k}\gamma}} = \sum_{\vec{k}}\frac{V^2}{\omega - \xi_{\vec{k}\gamma}} - i\pi V^2\sum_{\vec{k}}\delta(\omega - \xi_{\vec{k}\gamma}). \qquad (15)$$

The sum on $\vec{k}$ in the bidimensional space (k_x, k_y), which appears in Eq. (15), is transformed into an integral in the energy space. The density of states $\rho(\xi)$ is obtained from Eq. (6) and the usual relation $\sum_{\vec{k}} \to (1/2\pi^2)\int d\vec{k} = \int\rho(\xi)d\xi$. For each conduction band, labeled by $\gamma = \pm$, the density of states ρ_γ is written as

$$\rho_\gamma(\xi) = \rho_0\left(1 - \epsilon_\gamma\sqrt{\frac{\xi_R}{\xi + \xi_R}}\right)\theta(\xi) + (1 - \epsilon_\gamma)\rho_0\sqrt{\frac{\xi_R}{\xi + \xi_R}}\theta(-\xi)\theta(\xi + \xi_R), \quad (16)$$

where $\rho_0 = m/(2\pi\hbar^2)$ is the density of state of the conduction band of a bidimensional system, without the Rashba effect, $\theta(x)$ is the Heaviside step function defined as $\theta(x) = 1$ for $x \geq 0$ and zero otherwise. With the above considerations and assuming the bandwidth to be equal to D, the function $\Sigma^\gamma(\omega)$ that appears in Eqs.(13) and (14) is rewritten as

$$\Sigma^\gamma(\omega) = \mathrm{Re}\,\Sigma^\gamma(\omega) + i\,\mathrm{Im}\,\Sigma^\gamma(\omega) \qquad (17)$$

4

where

$$\text{Im}\,\Sigma^{\gamma}(\omega) = -\Gamma\left[\left(1 - \epsilon_{\gamma}\sqrt{\frac{\xi_R}{\omega + \xi_R}}\right)\theta(\omega) + (1 - \epsilon_{\gamma})\sqrt{\frac{\xi_R}{\omega + \xi_R}}\theta(-\omega)\theta(\omega + \xi_R)\right],\tag{18}$$

$\Gamma = \pi\rho_0 V^2$, and for $\omega + \xi_R \geq 0$,

$$\text{Re}\,\Sigma^{\gamma}(\omega) = \gamma\frac{\Gamma}{\pi}\sqrt{\frac{\xi_R}{\omega + \xi_R}}\left[\ln\left|\frac{\omega + \xi_R - \sqrt{(D + \xi_R)(\omega + \xi_R)}}{\omega + \xi_R + \sqrt{(D + \xi_R)(\omega + \xi_R)}}\right|\right.$$
$$\left. - \ln\left|\frac{\omega + \xi_R - \sqrt{\xi_R(\omega + \xi_R)}}{\omega + \xi_R + \sqrt{\xi_R(\omega + \xi_R)}}\right|\right] + \frac{\Gamma}{\pi}\ln\left|\frac{\omega}{\omega - D}\right|$$
$$+ (1 - \epsilon_{\gamma})\frac{\Gamma}{\pi}\sqrt{\frac{\xi_R}{|\omega + \xi_R|}}\ln\left|\frac{\omega + \xi_R + \sqrt{\xi_R(\omega + \xi_R)}}{\omega + \xi_R - \sqrt{\xi_R(\omega + \xi_R)}}\right|,\tag{19}$$

and for $\omega + \xi_R < 0$,

$$\text{Re}\,\Sigma^{\gamma}(\omega) = \gamma\frac{2\Gamma}{\pi}\sqrt{\frac{\xi_R}{|\omega + \xi_R|}}\tan^{-1}\left[\frac{(\sqrt{D + \xi_R} - \sqrt{\xi_R})\sqrt{|\omega + \xi_R|}}{|\omega + \xi_R| + \sqrt{(D + \xi_R)\xi_R}}\right]$$
$$- (1 - \epsilon_{\gamma})\frac{2\Gamma}{\pi}\sqrt{\frac{\xi_R}{|\omega + \xi_R|}}\tan^{-1}\left[\frac{\sqrt{|\xi_R|}}{\sqrt{|\omega + \xi_R|}}\right] + \frac{\Gamma}{\pi}\ln\left|\frac{\omega}{\omega - D}\right|.\tag{20}$$

Hence, introducing Eqs.(13) and (14) into the Fourier transform of Eqs. (10) and (11), finally we obtain

$$G^R(c_{f\uparrow};\omega) = \frac{1}{2}\sum_{\gamma}\left[\frac{1}{\omega - \Delta_+ - \Sigma^{\gamma}(\omega) - \Delta_-^2\left[\omega - \Delta_+ - \Sigma^{-\gamma}(\omega)\right]^{-1}}\right.$$
$$\left. + \frac{\Delta_-}{\prod_{\gamma}[\omega - \Delta_+ - \Sigma^{\gamma}(\omega)] - \Delta_-^2}\right]\tag{21}$$

$$G^R(c_{f\downarrow};\omega) = \frac{1}{2}\sum_{\gamma}\left[\frac{1}{\omega - \Delta_+ - \Sigma^{\gamma}(\omega) - \Delta_-^2\left[\omega - \Delta_+ - \Sigma^{-\gamma}(\omega)\right]^{-1}}\right.$$
$$\left. - \frac{\Delta_-}{\prod_{\gamma}[\omega - \Delta_+ - \Sigma^{\gamma}(\omega)] - \Delta_-^2}\right].\tag{22}$$

Eqs. (21) and (22) provide the spectral function $A(c_{f\nu};\omega)$, given by

$$A(c_{f\nu};\omega) = -2\,\text{Im}\,G^R(c_{f\nu};\omega),\tag{23}$$

and the occupation of the impurity orbital, $\langle n_{f\nu}\rangle = \left\langle c_{f\nu}^{\dagger}c_{f\nu}\right\rangle$, written as

$$\langle n_{f\nu}\rangle = \int\frac{d\omega}{2\pi}A(c_{f\nu};\omega)\eta_F(\omega),\tag{24}$$
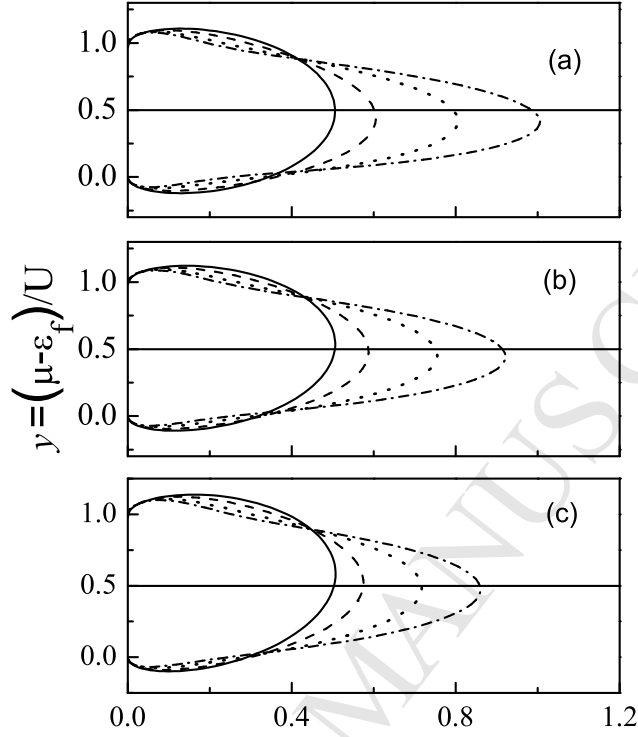
5

Figure 1: Boundary between magnetic and non-magnetic phase in the variables $x = \pi\Gamma/2U$ and $y = (\mu - \epsilon_F)/U$ for $\xi_R = 0.0$ (solid-line), $\xi_R = 0.1$ (dashed-line), $\xi_R = 0.3$ (dotted-line) and $\xi_R = 0.5$ (dashed-dotted-line) in (a) μ=0.5, (b) μ=0.6 and (c)μ=0.7.

where $\eta_F(\omega)$ is the Fermi distribution function. The magnetization m can be obtained from $m = \langle n_{f\uparrow}\rangle - \langle n_{f\downarrow}\rangle$,which will be analyzed in the next section.

The adimensional conductance can be calculated by

$$G/G_0 = \sum_\nu \int d\omega \rho_{f\nu}(\omega) \left[n_F(\omega) - n_F(\omega + eV)\right] \qquad (25)$$

4. Results and Discussion

In this section we present the phase diagram of the Rashba dot as a function of the parameters $x = \pi\Gamma/2U$ and $y = (\mu - \epsilon_f)/U$ utilizing Eq. (24) and also the chemical potential dependencies of the occupation numbers $\langle n_{f\uparrow}\rangle$ and $\langle n_{f\downarrow}\rangle$ as well as the electrical conductance through the impurities.

In Fig. 1, the phase diagrams are discussed for $\xi_R = 0.0$ (solid-line), $\xi_R = 0.1$ (dashed-line), $\xi_R = 0.3$ (dotted-line) and $\xi_R = 0.5$ (dashed-dotted-line) in (a)

μ=0.5, (b) μ=0.6 and (c) μ=0.7. For the sake of numerical calculations we utilize $\Gamma = 0.01$ and all the parameters are given in terms of the bandwidth if not mentioned otherwise. For $\xi_R = 0.0$ we observe the magnetic to non-magnetic phase diagram to be symmetric around $y = 0.5$ as seen in metals without Rashba coupling [40]. However, in the presence of the Rashba interaction, there is a variation in the symmetry of the transition line and also an increase in the magnetized region with the increase in the Rashba coupling. The boundary is asymmetric in all the cases for $\xi_R > 0.0$. The limits of the y values of the magnetized phase continue to be the same at $x = 0$ when compared to the metallic case without Rashba coupling. Nevertheless, for $x > 0$ a change in the symmetry of the boundary line around $y = 0.5$ is evident. Nonetheless, the effect in the magnetized region along the x-direction is more pronounced. The $x-$values increases for the magnetized region with an increase in ξ_R. The increase in the chemical potential nevertheless decreases the magnetic phase along the $x-$direction. As we can see from eq. (6) of the manuscript, the conduction band suffers a shift with respect to the Fermi energy due to the presence of the Rashba term and thereby affects the symmetry as well as the magnetic phase. The origin as well as the values in the dispersion relation are modified due to the insertion of the Rashba coupling.

In Fig. 2, the dependencies of the occupation numbers $\langle n_{f\uparrow} \rangle$ and $\langle n_{f\downarrow} \rangle$ of the impurity on the chemical potential μ are plotted for $\Gamma = 0.01$ in (a)$\epsilon_F = 0.2$, $U = 0.3$ (b) $\epsilon_F = 0.2$, $U = 0.5$ and (c)$\epsilon_F = 0.3$, $U = 0.5$. The dependencies are demonstrated for $\xi_R = 0.0$ (solid-line), $\xi_R = 0.5$ (dashed-line), $\xi_R = 1.0$ (dotted-line) in all the above cases. The $\xi_R = 0.0$ case, that represents the metallic case without Rashba coupling, is also exhibited for comparison with that in the presence of Rashba interaction. The presence of the Rashba coupling tends to shift the region of the local moment formation towards the right (higher values of μ). Moreover, the $\langle n_{f\uparrow} \rangle$ increases appreciably when compared to $\xi_R = 0.0$ case and thereby increases the magnetization values. As ξ_R increases the magnetization values also increases principally due to the increase in $\langle n_{f\uparrow} \rangle$. The $\langle n_{f\downarrow} \rangle$ suffers very little variation. An increase in the Coulomb interaction U in Fig. 2(b) increases the region of the magnetic moment formation. However, the magnetization values modifies very little. Comparing Fig. 2(b) and Fig. 2(c) we could verify the effect of the impurity energy of the dots on the local magnetic formation. Both the region of the moment formation and the magnetization decreases with the increase in ϵ_f. The magnetization m given by $m = \langle n_{f\uparrow} \rangle - \langle n_{f\downarrow} \rangle$ are exhibited for $\Gamma = 0.01$, $\xi_R = 0.0$ (solid-line), $\xi_R = 0.5$ (dashed-line), $\xi_R = 1.0$ (dotted-line) in (d)$\epsilon_F = 0.2$, $U = 0.3$ (e) $\epsilon_F = 0.2$, $U = 0.5$ and (f)$\epsilon_F = 0.3$, $U = 0.5$. The chemical potential dependencies of conductance values of the impurity are presented for $\Gamma = 0.01$, $\xi_R = 0.0$ (solid-line), $\xi_R = 0.5$ (dashed-line), $\xi_R = 1.0$ (dotted-line) in (g)$\epsilon_F = 0.2$, $U = 0.3$ (h) $\epsilon_F = 0.2$, $U = 0.5$ and (i)$\epsilon_F = 0.3$, $U = 0.5$. The conductance values presents two cusps at the critical point where the dot experiments a magnetic-non-magnetic transition. The peak values of the adimensional conductance is very little dependent on the parameters of the system. The position is dependent on the critical value of the chemical potential of the local moment formation.
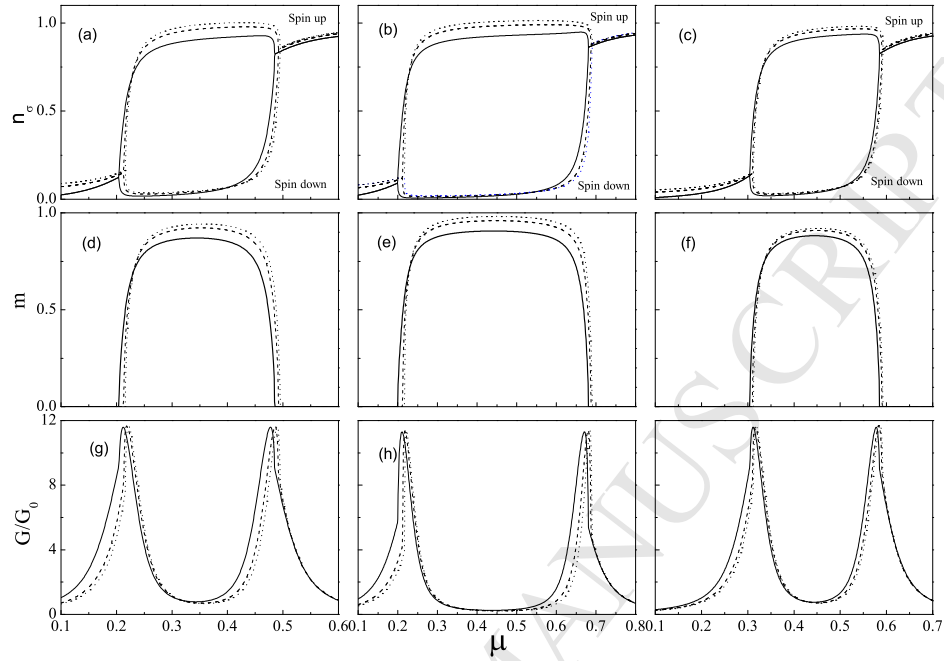
7

Figure 2: $n_{f\nu}$ vs μ for $\Gamma = 0.01$, $\xi_R = 0.0$ (solid-line), $\xi_R = 0.5$ (dashed-line), $\xi_R = 1.0$ (dotted-line) in (a)$\epsilon_F = 0.2$, $U = 0.3$ (b) $\epsilon_F = 0.2$, $U = 0.5$ and (c)$\epsilon_F = 0.3$, $U = 0.5$. Magnetization m=$\langle n_{f\uparrow} \rangle - \langle n_{f\downarrow} \rangle$ for $\Gamma = 0.01$, $\xi_R = 0.0$ (solid-line), $\xi_R = 0.5$ (dashed-line), $\xi_R = 1.0$ (dotted-line) in (d)$\epsilon_F = 0.2$, $U = 0.3$ (e) $\epsilon_F = 0.2$, $U = 0.5$ and (f)$\epsilon_F = 0.3$, $U = 0.5$, G/G_0 vs μ for $\Gamma = 0.01$, $\xi_R = 0.0$ (solid-line), $\xi_R = 0.5$ (dashed-line), $\xi_R = 1.0$ (dotted-line) in (g)$\epsilon_F = 0.2$, $U = 0.3$ (h) $\epsilon_F = 0.2$, $U = 0.5$ and (i)$\epsilon_F = 0.3$, $U = 0.5$

5. Conclusions

The Green's function equation of motion formalism was utilized to study the local moment formation and the adimensional conductance for a magnetic impurity in a metallic host in the presence of the Rashba coupling. The Coulomb interaction between the electrons in the magnetic impurity and the interaction of the dot with the conduction electrons were considered. The phase diagram depends on the Rashba interaction and also is sensitive to ϵ_F and U. Moreover, the occupation numbers also depend on the Rashba interaction that molds the adimensional conductance. The critical values of the chemical potential of the magnetic-non-magnetic transition correspond to the cusps in the G/G_0 curves.

References

[1] V. Joshi. Eng. Sci. Tech., 19, (2016), p.1503

[2] E. E. Fullerton, J. R. Childress, Proc IEEE, 104 (2016), p.1787.

[3] J. Fabian, A. Matos-Abiague, C. Ertler, P. Stano, I. Žutić Acta Phys. Slov. 57 (2007), p.565.

[4] G. E. W. Bauer, E. Saitoh, B. J. van Wees, Nature Mater., 11 (2012), p. 391–399,

[5] K. Uchida, S. Takahashi, K. Harii, J. Ieda, W. Koshibae, K. Ando, S. Maekawa, and E. Saitoh, Nature, 455 (2008) p. 778.

[6] S. O. Demokritov and A. N. Slavin, Magnonics: From Fundamentals to Applications. New York, USA: Springer-Verlag, (2013).

[7] C. Wang et al., J. Appl. Phys. 106, (2009), p.053905.

[8] J.-G. Zhu, X. Zhu, and Y. Tang, IEEE Trans. Magn., 44, (2008) p. 125.

[9] H. A. M. van den Berg, W. Clemens, G. Gieres, G. Rupp, W. Schelter, M. Vieth, IEEE Trans. Magn., 32 (1996) p. 4624.

[10] K. LePhan, H. Boeve, F. Vanhelmont, T. Ikkink, F. de Jong, H. de Wilde, Sensors Actuators A, 129 (2006), p. 69.

[11] S. X. Wang et al., J. Mag. Magn. Mat. 293, (2005) p. 731.

[12] J. Amaral et al., IEEE Trans. Magn., 49 (2013) p. 3512.

[13] S.A. Wolf et al., Science 294 , 1488 (2001).

[14] S. Wienholdt, D. Hinzke, U. Nowak Phys. Rev. Lett., 108 (2012), p. 247207

[15] A.H. MacDonald, M. Tsoi, Philos. Trans. R. Soc. A, 369 (2011), p. 3098

[16] S. Loth, S. Baumann, C.P. Lutz, D.M. Eigler, A.J. Heinrich, Science, 335 (2012), pp. 196-199

[17] P. Wadley, V. Novák, R.P. Campion, et al. Nat. Commun., 4 (2013), p. 2322

[18] Z. Wei, A. Sharma, A. Núñez, P.M. Haney, R.A. Duine, J. Bass, A.H. MacDonald, M. Tsoi, Phys. Rev. Lett., 98 (2007), p. 116603

[19] R. Cheng, J. Xiao, Q. Niu, A. Brataas, Phys. Rev. Lett., 113 (2014), p. 057601.

[20] R. G. Bhardwaj et al, Appl. Phys. Lett. 112, (2018) p.042404.

[21] Y. K. Kato, R. C. Myers, A. C. Gossard, and D. D. Awschalom, Science 306, (2004) p.1910.

[22] J. Wunderlich, B. Kaestner, J. Sinova, and T. Jungwirth, Phys. Rev.Lett. 94, (2005), p.047204.

[23] S. Murakami, N. Nagosa, and S.-C. Zhang, Science 301, (2003) p.1348.

[24] , J. Schliemann, D. Loss, and R. M. Westervelt, Phys. Rev. B 73, (2006) p.085323

[25] K. L. Wang et al., J. Phys. D, Appl. Phys. 46, (2013), p.074003.

[26] H. S. P. Wong and S. Salahuddin, Nature Nanotechnol. 10, (2015) p. 191.

[27] S. Datta and B. Das, Appl.Phys. Lett., 56 (1990), p.665

[28] J. Nitta, T. Akazaki, H. Takanayagi and T. Enoki, Phys. Rev. Lett. 78, (1997) p.1335; G. Engels, J. Lange, TH. Schapers and H. Luth, Phys. Rev. B, 55 (1997), p.R1958.

[29] J. C. Egues, G. Burkard and D. Loss Phys. Rev. Lett., 89 (2003), p.176401; J. C. Egues, G. Burkard, D. S. Saraga, J. Schliemann and D. Loss Phys. Rev. B, 72 (2005), p.235326.

[30] Miller, J. B. et al. Phys. Rev. Lett., 90 (2003), p.076807.

[31] S. Estévez Hernández, et al. Phys. Rev. B, 82 (2010), p.235303.

[32] Z. Scherübl, et al. Phys. Rev. B, 94 (2016), p.035444.

[33] K. Takase, Y. Ashikawa, G. Zhang, K. Tateno and S. Sasaki Scientific Reports, 7 (2017), p.930

[34] S. Tarucha, D. G. Austing, T. Honda, R. J. van der Hage and L. P. Kouwenhoven Phys. Rev. Lett., 77 (1996), p.3613

[35] L. P. Kouwenhoven, D. G. Austing and S. Tarucha Rep. Prog. Phys., 64 (2001), p.701

[36] P. Hawrylak, C. Gould, A. Sachrajda, Y. Feng, Z. Wasilewski, Phys. Rev. B, 59 (1999), p.2801.

[37] C. Gould, P. Hawrylak, A. Sachrajda, Y. Feng, P. Zawadzki, Z. Wasilewski Physica E, 6 (2000), p.461

[38] R. López and D. Sánchez and L. Serra Phys. Rev. B, 76 (2007), 035307

[39] M. Crisan, D. Sánchez, R. López L. Serra and I. Grosu Phys. Rev. B, 79 (2009), p.125319

[40] P. W. Anderson, Phys. Rev., 124 (1961), p. 41.